Studies of Cation Binding in $ZnCl_2$-Regenerated Bacteriorhodopsin by X-Ray Absorption Fine Structures: Effects of Removing Water Molecules and Adding Cl^- Ions

Ke Zhang,* Li Song,# Jun Dong,* and M. A. El-Sayed#
*Biostructures Institute, Philadelphia, Pennsylvania 19104-3358, and #School of Chemistry and Biochemistry, Georgia Institute of Technology, Atlanta, Georgia 30332-0400 USA

ABSTRACT The binding of Zn^{2+} in Zn^{2+}-regenerated bacteriorhodopsin (bR) was studied under various conditions by x-ray absorption fine structures (XAFS). The 0.9:1 and 2:1 Zn^{2+}:bR samples gave similar XAFS spectra, suggesting that Zn^{2+} might have only one strong binding site in bR. It was found that in aqueous bR solution, Zn^{2+} has an average of six oxygen or nitrogen ligands. Upon drying, two ligands are lost, suggesting the existence of two weakly bound water ligands near the cation-binding site in bacteriorhodopsin. When excess Cl^- ions were present before drying in the Zn^{2+}-regenerated bR samples, it was found that two of the ligands were replaced by Cl^- ions in the dried film, whereas two remain unchanged. The above observations suggest that Zn^{2+} has three types of ligands in regenerated bR (referred to as types I, II, and III). Type I ligands are strongly bound. These ligands cannot be removed by drying or by exchanging with Cl^- ions. Type II ligands cannot be removed by drying, but can be replaced by Cl^- ligands. Type III ligands are weakly bound to the metal cation and are most likely water molecules that can be removed by evaporation under vacuum or by drying with anhydrous $CaSO_4$. The results are discussed in terms of the possible structure of the strongly binding site of Zn^{2+} in bR.

INTRODUCTION

Bacteriorhodopsin (bR) is one of the two natural photosynthetic systems, the second being chlorophyll. bR is the only protein found in the purple membrane (PM) of *Halobacterium salinarium*. It was first discovered in 1971 by Oesterhelt and Stoeckenius (1971). The retinal chromophore of bR is covalently bound via a protonated Schiff base (-CN^+H-) (PSB) linkage to the ϵ-amino group of the Lys^{216} residue in the protein. Upon absorption of photons, light-adapted bR goes through a cyclic reaction involving a number of intermediates before returning to its initial state, bR_{568}. The photocycle can be summarized as follows:

$$bR_{568} \xrightarrow{h\nu} (bR)^* \xrightarrow{0.2ps} I_{460} \xrightarrow{0.5ps} J_{625} \xrightarrow{\sim 3ps} K_{610} \xrightarrow{2\mu s}$$

$$L_{550} \xrightarrow[-H^+]{70\mu s} M_{412} \xrightarrow[+H^+]{ms} N_{550} \rightarrow O_{640} \rightarrow bR_{568}$$

In the $L_{550} \rightarrow M_{412}$ step, a proton is transferred from the protonated Schiff base (PSB) to Asp^{85} (Braiman et al., 1988; Butt et al., 1989; Otto et al., 1990). At almost the same time, another proton appears on the extracellular surface (Dencher et al., 1991; Heberle and Dencher, 1992) of the membrane. As a result of the photocycle, protons are translocated across the cell membrane, establishing a pH gradient that is used for metabolic processes such as ATP synthesis (Lozier et al., 1976; Ort and Parson, 1978). M_{412} is the only intermediate in which the Schiff base is unprotonated during the photocycle. The pK_a value of the PSB is 13.3 in bR_{570} (Druckmann et al., 1982; Sheves et al., 1986). However, the fact that M_{412} is formed even when the pH of the medium is below 3 suggests a large reduction in the pK_a value of the PSB during the photocycle (Chronister et al., 1986).

Well-washed PM contains only Ca^{2+} and Mg^{2+} (Chang et al., 1985; Griffiths et al., 1996a). Removal of these cations from PM by ion exchange (Chang et al., 1985) or acidification (Oesterhelt and Stoeckenius, 1971; Kobayashi et al., 1983) causes a color transition from purple (570 nm) to blue (606 nm). Although photoisomerization of the retinal takes place in blue bR, it does not form the M_{412} intermediate, and thus does not pump protons (Chang et al., 1985). Different models have been proposed regarding the binding of metal cations and how they control the color of the purple membrane. Szundi and Stoeckenius (1987, 1988, 1989) treated the metal ions as free positive charges distributed uniformly on the membrane surface that regulate the surface pH via the Gouy-Chapman effect. In this model the removal of the cations increases the negative surface charge density, which in turn lowers the surface pH. This pH change causes the protonation of the aspartate counterion(s), which affects the color of retinal. Several other groups (Ariki and Lanyi, 1986; Chang et al., 1986; Dunach et al., 1988a,b; N. Y. Zhang et al., 1992) emphasize the existence of specific chemical binding between some of the metal cations and the negatively charged groups (e.g., carboxylate groups of Asp) within the protein.

Numerous experiments have been carried out to investigate the locations of the metal cations in bR. Calcium binding in bR was studied with a calcium-sensitive elec-

Received for publication 13 September 1996 and in final form 17 June 1997.

Address reprint requests to Dr. Mostafa A. El-Sayed, Department of Chemistry and Biochemistry, Georgia Institute of Technology, Atlanta, GA 30332. Tel.: 404-894-0292; Fax: 404-894-0294; E-mail: mostafa.el-sayed@chemistry.gatech.edu.

© 1997 by the Biophysical Society

0006-3495/97/10/2097/09 $2.00

trode (N. Y. Zhang et al., 1992; Zhang and El-Sayed, 1993). It was found that there are two strong binding sites located within the protein. The high-affinity binding sites are proposed to be stabilized by the negative charges of Asp^{85} and Asp^{212} located near the retinal pocket (Jonas and Ebrey, 1991; Zhang et al., 1993). In addition, there are several weaker metal cation-binding sites that appear to be located mostly on the cytoplasmic surface of the protein.

Several attempts have been made to locate metal cations in bR by using x-ray diffraction and electron diffraction techniques. Studies on Pb^{2+}-regenerated bR films (Katre et al., 1986; Mitra and Stroud, 1990) indicate that up to four distinct binding sites are located on the α-helices of the protein. In another study (Englehard et al., 1987), XAFS of Fe^{3+} was carried out to investigate the binding environment of the Fe^{3+} cations in bR. The results (Englehard et al., 1987) suggest an octahedral geometry for the metal ions with 5.8 ± 1.5 ligands. A second coordination shell was found in the Fe^{3+}-regenerated bR. A more recent XAFS study on Mn^{2+}-regenerated bR (Sepulcre et al., 1996) suggests that the mechanisms of binding of Mn^{2+} in bR and in water are very similar. In addition, it was reported that the second shell observed in Fe^{3+}-regenerated bR (Englehard et al., 1987) was missing in Mn^{2+}-regenerated bR (Sepulcre et al., 1996). Recent publications on the binding of rare earth ions to deionized bR suggest that the binding site differs from that for Ca^{2+}, in that it has strong affinity for bidentate binding to the PO_2^- groups of the lipids (Griffiths et al., 1996b). From the near-infrared vibronic side band spectroscopy of Yb^{3+}, it was concluded that in addition to binding to the PO_2 groups of the phospholipids, the rare earth Yb^{3+} also binds to the protein residues at the same time (Roselli et al., 1996). It thus seems possible that the structure of the binding site might depend on the metal cations used.

We have performed a systematic study to examine the metal environment of Zn^{2+}-regenerated bR using x-ray absorption fine structure (XAFS) in bR solutions as well as in bR films under various conditions for 0.9:1 and 2:1 Zn^{2+}:bR (to determine whether Zn^{2+} has more than one different strong binding site in bR). We chose to use Zn^{2+} for the following reasons: 1) Zn^{2+}-regenerated bR showed very similar M_{412} formation and decay kinetics compared to the wild-type bR. 2) Zn^{2+} is divalent and does not have valence *d* electrons; thus Zn^{2+} is similar to Ca^{2+} and Mg^{2+}, which are found in the wild-type bR. 3) The XAFS of Zn^{2+} is much easier to obtain by using currently available x-ray sources at Brookhaven National Laboratories than the native Ca^{2+} and Mg^{2+} cations in wild-type bR. By comparing the XAFS of Zn^{2+} under various conditions (aqueous solution, dry and wet films, dry film with excess Cl^- ions), changes in the number of ligands and the average distance between the Zn^{2+} cation and its ligands under different conditions are revealed. Our results provide new insights into the coordination(s) of metal cations with the binding sites in bR.

MATERIALS AND METHODS

The purple membrane was obtained and purified according to a combination of methods outlined previously (Oesterhelt and Stoeckenius, 1974; Becher and Cassim, 1975). Deionized blue bR was obtained by running the purple membrane through a Bio-Rad AG 50W-X4 (Richmond, CA) column of cation exchanger in its hydrogen form (Corcoran et al., 1987). A 5 mM solution of $ZnCl_2$ was added to a solution of blue bR with known concentration and volume. The number of Zn^{2+} per bR is a nominal ratio calculated from the measured volumes and known concentrations of $ZnCl_2$ and bR. Based on previous studies on divalent cation binding to deionized bR, these nominal ratios are very close to the number of bound metal cations per bR (N. Y. Zhang et al., 1992; Yoo et al., 1995). The samples were then left at room temperature overnight before any pH adjustment was made. The pH of the solutions was adjusted to ~6 by using 1 mM KOH solution or by using a 100 mM phosphate buffer. No difference in the XAFS spectrum was observed between samples whose pH was adjusted with KOH and those whose pH were adjusted with the phosphate buffer. After the pH adjustment, the samples were left at room temperature for ~4 h. Then the samples were washed with ~20 ml of doubly deionized water. bR was pelleted out by centrifugation at 19,000 rpm for 30 min.

To make bR samples with excess Cl^- ions, KCl was added to the buffer solution with a final concentration of ~100 mM KCl in 100 mM phosphate buffer. The final concentration of Cl^- in the Zn^{2+}-regenerated bR solutions was ~10 mM. The Zn^{2+}-regenerated bR solutions were washed with only 1 ml of doubly deionized water, followed by pelleting in a centrifuge.

To prepare Zn^{2+}-regenerated bR samples in solution, the bR pellet obtained from centrifugation was mixed with ~200 μl of doubly deionized water. After good mixing, the bR sample was transferred to a sample holder (a Teflon block with a 40 mm × 2 mm × 2 mm slit), which was then sealed with Mylar tape. To prepare bR films, bR solution was first transferred into a sample holder and then slowly dried under 80% relative humidity over 12 h. To get a wet film, the bR film was equilibrated with deionized water for 10 h before the XAFS experiments. To get a dry film, the bR film formed under 80% relative humidity was either dried under vacuum with a mechanical pump (10 μTorr pressure) for a few hours or under anhydrous $CaSO_4$ in an airtight container for more than 24 h before the XAFS measurements. No significant differences were observed between samples that were dried using these two different techniques.

All of the XAFS measurements were carried out at Beamline X9-B of the National Synchrotron Light Source, Brookhaven National Laboratory. The single wavelength x-ray beam was selected by using a Si (220) double-crystal monochromator with a constant exit height, and a Ni-plated harmonic rejection mirror placed downstream. The fluorescence signal emitted after the x-ray absorption was collected with a 13-element Ge detector. The individual energy windows of the detector were carefully set to maximize the effective signal counts. The detector dead time was calibrated on individual samples and corrected with a simple algorithm (K. Zhang et al., 1992b). The incident count rate of each detector element was maintained at 40–60% of its saturation level, which is ~70,000, to ensure a reliable correction.

XAFS of all bR samples were measured at room temperature. Zn^{2+}-regenerated bR films were measured under dry and wet conditions. In the former case, dry helium or nitrogen gas was supplied to the sample chamber, whereas in the latter case water was sealed in the chamber, and/or wet gas was supplied to the chamber by bubbling He gas through a water bubbler. The final concentration of the protein was generally 1–2 mM. A series of scans were collected for each sample, with total signal counts of several million per data point. Fine crystalline powder of metal complexes, $ZnAc_2Im_2$ (Horrocks et al., 1980), ZnO, and ZnS, was also measured under the same experimental conditions.

The absorption data collected were reduced to an XAFS χ function by techniques described previously (K. Zhang et al., 1992a). Fourier transform was applied to the XAFS χ data to obtain a pseudoradial distribution function in *R*-space. The atomic distributions of interest, usually the first coordination sphere, were selected by back-transform to *k*-space with a window function.

Empirical model compounds, $ZnAc_2Im_2$, ZnO, and ZnS, were used for deriving the structural parameters from the experimental data. $ZnAc_2Im_2$, with two nitrogens and two oxygens located at an average distance of 1.986 Å from the zinc, has been proved to be a good empirical standard to model Zn-O and Zn-N contributions (K. Zhang et al., 1992a). It is expected that ZnS can be used to model the Zn-Cl bond, in addition to Zn-S bonds, because of the similarity of the scattering properties of Cl and S. The validity of modeling Zn-Cl with Zn-S bonds has been tested by using theoretical standards from the FEFF program (Mustre de Leon et al., 1991). Fitting of the Zn-Cl standard with the Zn-S standard obtained an error of 2% in coordination number and 0.02 Å in interatomic distance.

Using phase and amplitude functions derived from empirical models, least-squares fitting was performed on the isolated single-shell χ data. Proper error analysis is essential for evaluating the fitting results in particular on dilute systems. We have been using a criterion to determine whether a fit should be accepted or rejected based on the value of Q (Zhang et al., 1988):

$$Q = \frac{1}{N-P}\sum_{i}^{N}\frac{(\sigma_f^i)^2}{(\sigma_y^i)^2}$$

where

$$(\sigma_f^i)^2 = (A^i)^2(\phi^i - \phi_f^i) + (A^i - A_f^i)^2$$

Here A^i and ϕ^i are the experimental amplitude and phase determined at the independent data point of k_i, and A_f and ϕ_f are the corresponding values of the fit. N is the number of independent data points included within the data range to be modeled (Lee et al., 1981), and P is the number of parameters used in the fit. σ_y^i comprises measurement errors and errors introduced from the nontransferability of the standards to the unknown. Alternatively, the data were used to generate radial distribution functions (RDFs) by extrapolating the data down to $k = 0$ with cumulative expansion (Crozier et al., 1988; Stern et al., 1992). The RDF technique not only provides a reliable check for the fitting results, but also determines the structure with better resolution due to the low-k extrapolation.

RESULTS AND DISCUSSION

Fig. 1 compares the near-edge x-ray absorption spectra for bR protein containing 0.9 Zn^{2+} atom per molecule of bR in solution and in a film measured under dry and wet conditions. The pH of these samples was adjusted with a 100 mM phosphate buffer that contains 100 mM KCl. The spectral features of Zn^{2+} in bR solution are very similar to those in the wet bR film, while differing from those of the dry film. We have also tried to determine whether the effect is reversible, by rehydrating a dry bR film in a wet chamber. Time-dependent transitions from dry film to wet film spectra and vice versa (when the wet film was dried in the XAFS chamber) were observed. No difference in the XAFS spectrum was observed in bR solution or in wet bR films when 1 mM KOH was used to adjust the pH instead of the phosphate buffer containing 100 mM Cl^- ions. Significant changes, however, were observed in dry bR films when the pH was adjusted to ~6 with the phosphate buffer containing 100 mM KCl, compared to when the pH was adjusted with KOH or the phosphate buffer without KCl. This comparison is shown in Fig. 1.

Fig. 2, *A* and *B*, compares the near-edge spectra of bR sample containing 2.0 Zn^{2+}/bR with that containing 0.9 Zn^{2+}/bR in solution and in dry films with Cl^- ions. The

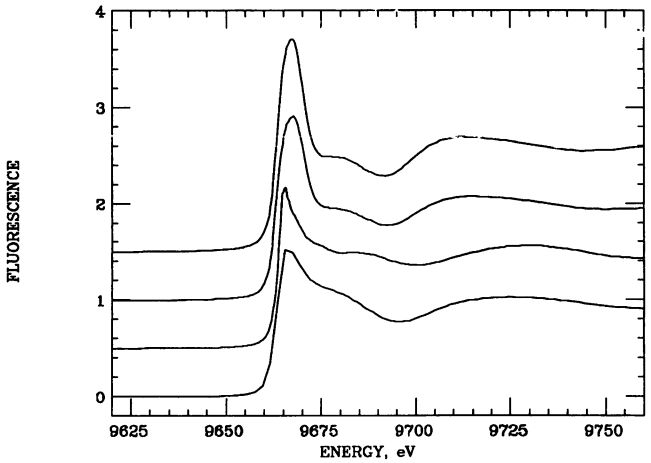

FIGURE 1 The x-ray absorption near edge spectra of Zn^{2+} in Zn^{2+}-regenerated bR containing 0.9 Zn^{2+} per bR molecule. Plotted here, from top to bottom, are the spectra of Zn^{2+} in Zn^{2+}-regenerated bR in aqueous solution, in a wet film, in a dry film in the presence of excess of Cl^{-1} ions, and in a dry film without Cl^{-1} ions. The spectra are obtained by pre-edge subtraction and by a normalization to the edge steps.

spectra are almost identical, indicating that the two zinc sites are very similar. This could suggest that Zn^{2+} has only one type of strong binding site in bR. As observed for the 0.9 Zn^{2+}/bR, spectral changes do occur when the sample is dehydrated for the 2.0 Zn^{2+}/bR sample. The XAFS functions derived from the absorption spectra are compared in Fig. 3 for 2.0 Zn^{2+}/bR in solution and in dry films. The two film samples shown were prepared differently: the pH of one was adjusted with a phosphate buffer without Cl^- ions, whereas the pH of the other was adjusted with a phosphate buffer that contained 100 mM Cl^- ions. From Fig. 3 it can be seen that the spectrum of 2.0 Zn^{2+}/bR in the solution differs from that in the dry film. In addition, the XAFS spectra of 2.0 Zn^{2+}/bR in the two dry films (with and without Cl^- ions) are also different (Fig. 3). These differences in the χ data for these samples can be examined by their Fourier transforms, which are shown in Fig. 4. The first coordination peak located at 1.5 Å for the solution sample shifted to 1.4 Å for the dry film sample without Cl^- ions, and shifted to 1.65 Å for the dry film sample with Cl^- ions.

The first coordination distributions shown in Fig. 4 were back-transformed to k-space by using a window function from 0.7 to 2.1–2.3 Å. Least-squares fitting was performed on the first shell χ data to derive structural parameters for Zn^{2+} in regenerated bR. The fitting results, which can be accepted based on whether the quantity Q is less or close to unity, are listed in Table 1. The first coordination shell of Zn^{2+} in bR can be modeled with six nitrogen or oxygen atoms located at an average distance of 2.07 ± 0.02 Å away from the Zn^{2+}. The distribution, which is somewhat disordered, is characterized by an XAFS Debye-Waller factor σ^2 of 0.005 $Å^2$ relative to that of the model complex. The first shell of Zn^{2+} in the dry film without Cl^- ions is found to

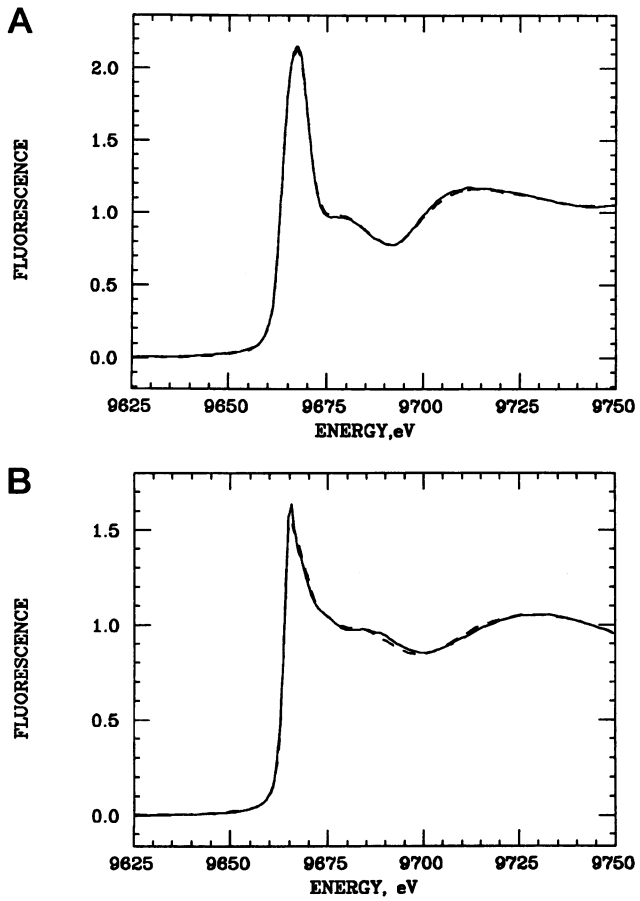

FIGURE 2 (*A*) The x-ray absorption near edge spectra of bR in aqueous solution containing 0.9 Zn^{2+} (——) and 2.0 Zn^{2+} (– – –) per bR molecule. (*B*) The x-ray absorption near edge spectra of bR in a dry film with Cl^- ions containing 0.9 Zn^{2+} (——) and 2.0 Zn^{2+} (– – –) per bR molecule.

contain four N/O atoms located at 1.97 ± 0.01 from the metal ion. When Cl^- ions are present, however, the first shell structure of Zn^{2+} in bR in the dry film changes substantially. Its first shell χ data cannot be modeled exclusively with a single-shell N/O atom. Modeling of the data with two subshells of N/O atoms also results in unacceptable fits, with Q values as large as 15. Fitting the data with one chlorine and three oxygen atoms yielded a Q value of 5, and fitting with three chlorine and one oxygen atoms yielded a Q value of 4. Thus the best-fitting result is obtained with two oxygen and two chlorine atoms. Examination of the real and imaginary parts of the Fourier transform indicates the presence of Cl ligands. Thus the first coordination shell of Zn^{2+} in a dry bR film with Cl^- ions present is best modeled with two subshells of N/O and Cl^- ligands. A good fit is obtained when we assume that two N/O atoms are located at 2.01 ± 0.02 Å and two Cl^- atoms are located at 2.28 ± 0.02 Å.

Although the data analysis cannot definitively distinguish between oxygen and nitrogen ligands, it suggests that the ligands of Zn^{2+} metal cation are primarily oxygen atoms based on the following considerations. Examination of the

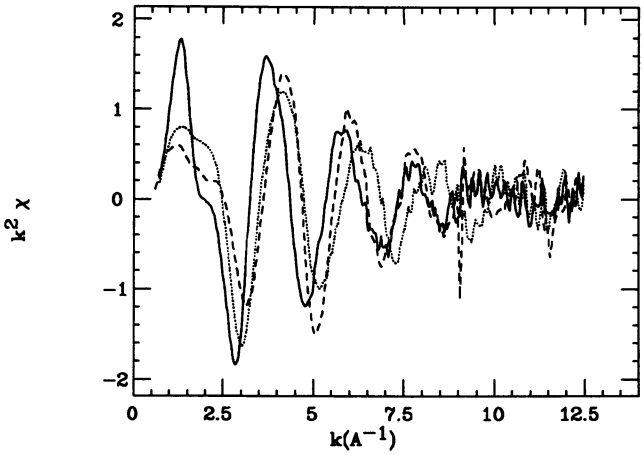

FIGURE 3 The XAFS $\chi(k)$ function for bR containing two Zn^{2+} per bR in aqueous solution (——) and in a dry film prepared with (– – –) and without (·····) the presence of excess Cl^- ions. The spectra are weighted with a k^2 factor.

Fourier transforms of the bR samples (Fig. 4) found reduced and displaced distributions, especially for the dry bR film with Cl^- ions. The four O or N ligands in the dry bR film without Cl^- ions are found at an average distance of 1.95 Å from the metal. This is shorter than that for a mixture of N or O ligands (Horrocks et al., 1980), in which the two oxygen ligands from two carboxylates are at 1.96 Å and the two imidazoles are at 2.01 Å from the metal cation.

The first shell radial distribution functions are generated by the "splice method" on various bR samples (Fig. 5 *A*). The method is less dependent on a preassumed structural model; thus it can be used to verify the fitting results. The RDF of the solution bR is found to contain approximately six N/O atoms, located at ~2.10 Å, whereas the RDF of the dry film bR without Cl^- ions contains about four N/O atoms located at 1.98 Å, which are consistent with the fitting results. The RDF of the dry bR film with Cl^- ions generated using the $ZnAc_2Im_2$ metal complex is unrealistic because of

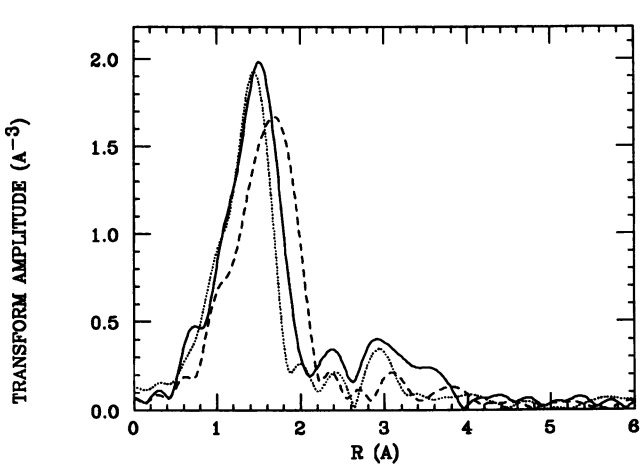

FIGURE 4 Fourier transforms of the k^2 $\chi(k)$ data shown in Fig. 2. The transforms were performed between 0.8 and 12.5 Å^{-1} in k-space.

TABLE 1 XAFS fitting results for the coordination number and the ligand distance in the first coordination sphere of Zn^{2+} in regenerated bR

	N or O ligands			Cl or S ligands			
2 Zn/bR Sample	CN	R (Å)	$\Delta\sigma^2$ (Å^2)	CN	R (Å)	$\Delta\sigma^2$ (Å^2)	Q
Solution	6.0 (6)	2.07 (2)	0.005	—	—	—	1.2
Dry film with Cl	2.0 (4)	2.01 (2) 11	−0.002	2.2 (4)	2.29 (2)	0.001	0.7
Dry film without Cl	4.0 (5)	1.95 (1)	0.000				1.0

The values in the bracket are the ± errors of the last digit. CN, Coordination number.

the presence of a large negative peak located at 2.3 Å (Fig. 5 *B*). Assuming the mixture of the signal from these atoms, the large negative peak can be attributed to the scattering phase difference between Cl/S and N/O atoms (Webster et al., 1991). Indeed, once the contribution of two N/O atoms is subtracted out, the residual RDF generated contains ~2.3 Cl atoms located at 2.27 Å (Fig. 5 *B*), which is consistent with the fitting results.

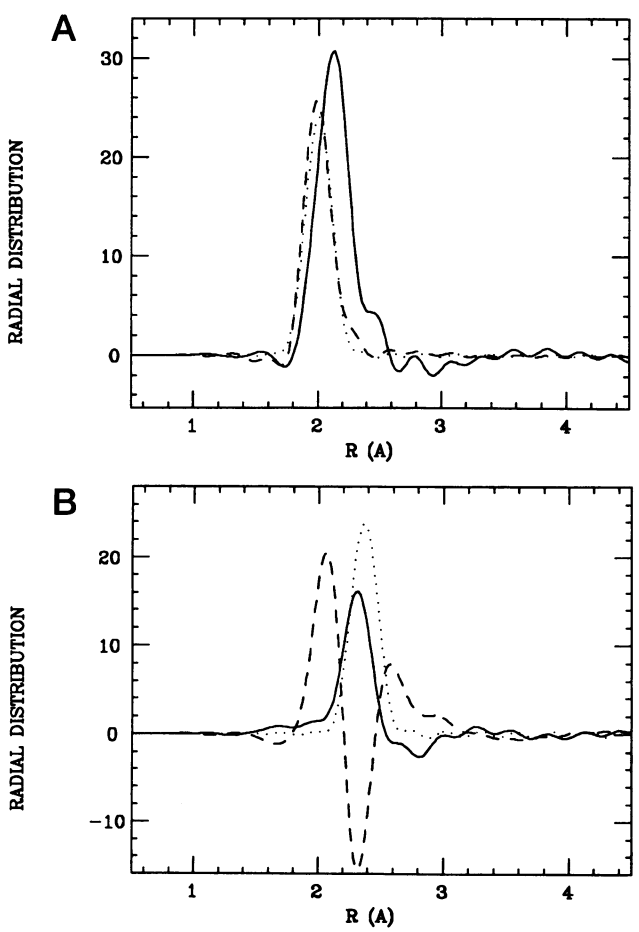

FIGURE 5 (*A*) The radial distribution functions (RDF) of bR containing two Zn^{2+} in aqueous solution (——) and in a dry film without Cl^- ions (– – –) are compared with the calculated RDF of $Zn(Ac)_2(Im)_2$ (·····), which is used as the model compound. (*B*) The RDFs of bR containing two Zn^{2+} in a dry film with Cl^- ions obtained by subtracting the contribution of two N/O atoms at 2.01 Å (——) is compared with the calculated RDF of ZnS (·····), which is used as the model compound. Also plotted here is the RDF of two Zn^{2+}/bR in a dry film with Cl^- ions generated, with $Zn(Ac)_2(Im)_2$ as the model compound (– – –). All of the distributions were broadened by a Gaussian factor of $\sigma^2 = 0.01$ Å^2 to reduce the truncation effects.

To verify that the changes in the dry film spectra are Cl^- concentration dependent, we measured a bR film sample with a low concentration of Cl^- under dry conditions. The analysis of this spectrum shows four O/N atoms in the first coordination shell, consistent with the results for dry bR film without Cl^- ions. After this measurement, the dry bR film sample was immersed in 100 mM KCl solution for several hours and remeasured under dry conditions. Again, the first shell was found to contain two O or N ligands and two Cl^- ligands, as found for dry bR, which was prepared with the phosphate buffer containing Cl^- ions.

Our first shell results for bR solution are in general agreement with the previous XAFS experiments on Fe^{3+}- and Mn^{2+}-regenerated bR samples. It was found (Englehard et al., 1987) that the iron atom is coordinated with 5.8 ± 1.5 oxygen atoms, with an average distance of 1.97 ± 0.02 Å. In a more recent study on the binding of Mn^{2+} to the high-affinity binding site of bR (Sepulcre et al., 1996), it was found that Mn^{2+} was coordinated to six oxygen atoms located at 2.17 Å. Unlike Fe^{3+}-regenerated bR, which showed an intense peak at 2.4/2.8 Å in the Fourier transform, the latter experiment (Mn^{2+}-regenerated bR) showed a rather small second coordination peak, consistent with our observation (Fig. 4). The cause of the difference was attributed to the trivalent Fe cation used instead of a divalent Mn^{2+} cation (Sepulcre et al., 1996). In the case of Zn^{2+}-regenerated bR, there was no difference found in the M-formation and decay kinetics (data not shown here). Thus it is reasonable to assume that Zn^{2+} does not change the nature of the binding site significantly. These results are consistent with experimental results, which suggest that trivalent cations form a bidentate complex with the PO^{2-} headgroups of the lipids, whereas the divalent cations do not (Petersheim et al., 1989; Roselli et al., 1996).

The near-edge spectrum of 0.9 Zn^{2+}/bR solution is compared with that of 2 mM $ZnCl_2$ solution (without bR) in Fig. 6. It is evident that the two samples are different both at the edge as well as in the XAFS region, suggesting that the binding of zinc cations with bR does occur. XAFS data analysis of the $ZnCl_2$ solution spectrum indicates that Cl^- binds to Zn^{2+}. This is in contrast to the Mn^{2+}-regenerated bR EXAFS results (Sepulcre et al., 1996), in which the spectrum of Mn^{2+} in aqueous solution showed great similarity to the Mn^{2+}-bR complex.

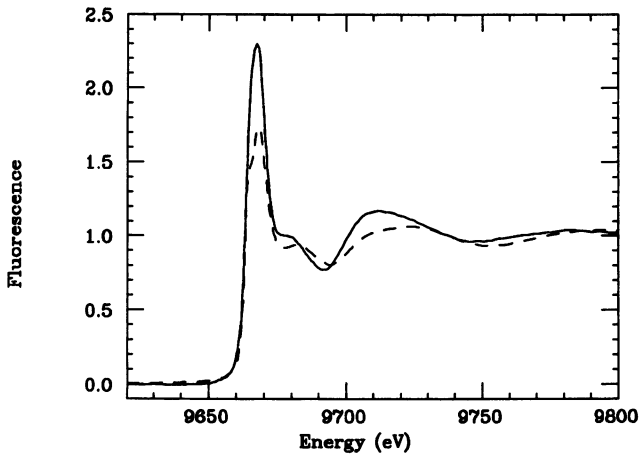

FIGURE 6 The x-ray absorption near edge spectra for bR proteins containing 0.9 Zn^{2+} per bR (——) compared with that of 2 mM $ZnCl_2$ aqueous solution (– – –). The coordination number of Zn^{2+} in 2 mM $ZnCl_2$ solution is 4 of oxygen and 2 of chlorine with average distances of 2.08 Å and 2.29 Å, respectively.

Few structural changes are found between samples with approximately one and two Zn^{2+} per bR for both bR solution and films. Various methods, such as electron spin resonance spectroscopy (Dunach et al., 1988a) for Mn^{2+}, filtration techniques for Ca^{2+} and Hg^{2+} (Dunach et al., 1988b), steady-state fluorescence methods for Eu^{3+} (Sweetman and El-Sayed, 1991), and potentiometric titration using specific Ca^{2+} electrodes (N. Y. Zhang et al., 1992), have all been employed to measure the binding constants for deionized bR with different cations. Calcium binding studies (N. Y. Zhang et al., 1992; Zhang and El-Sayed, 1993) provide evidence of two strong binding sites located in the protein. It was found that the second highest binding affinity site is responsible for the absorption shift (Ariki and Lanyi, 1986). It was also suggested that the binding site of the metal cation is composed of the protonated Schiff base, Asp^{85}, Asp^{212}, Y^{185}, Y^{57}, and R^{82} (Jonas and Ebrey, 1991). A more recent two-photon visible absorption study has suggested that three water molecules and four amino acid residues (Asp^{85}, Asp^{212}, Tyr^{57}, and Tyr^{185}) must be near the chromophore as well as close to an adjacent calcium-binding site (Stuart et al., 1995) to explain the observed two-photon visible absorption spectrum of bR.

A recent high-sensitivity electron diffraction study suggests that all of the high-affinity binding sites are within the protein, not in the phospholipids (Mitra and Stroud, 1990). ESR studies (Dunach et al., 1987) have suggested the existence of five high-affinity binding sites that are located near the protein carboxyl groups and five low-affinity binding sites that are close to the C-terminal segment. An octahedral coordination environment was suggested for the metal-binding site based on the inability of Hg^{2+} and Pt^{4+} to regenerate the spectral shift (Ariki and Lanyi, 1986) observed for other metal cations after mixing the metal cations with the deionized bR. The proximity of the metal cation to the retinal chromophore was also evident in the fluorescence study of Eu^{3+}-regenerated bR (Sweetman and El-Sayed, 1991). It was also shown that the trivalent cation binds more strongly to deionized bR than do the divalent cations; and the latter bind more strongly than the monovalent cations (Chang et al., 1985, 1986; Ariki and Lanyi, 1986). The above experimental results suggest the following: 1) There are different binding sites for metal cations in bR. 2) The high-affinity binding site are within the protein close to the retinal chromophore, but not on the surface of the phospholipids.

In a more recent study, it was shown (Yoo et al., 1995) that the binding constant of the first high-affinity binding site of Mg^{2+} is smaller than that of Ca^{2+}. The binding constant of the second affinity site of Mg^{2+} is similar to that of the first binding site. These observations suggest that the binding constant is affected by the nature of the divalent cations (such as their charge density, their hydration enthalpy, etc.). The preference of Ca^{2+} over Mg^{2+} in the first high-affinity binding site is due to the higher binding constant of Ca^{2+}. In addition, it was found that the two high-affinity binding sites are independent of each other (Yoo et al., 1995). From this (Yoo et al., 1995) and other studies (Chang et al., 1985, 1986) it can be concluded that the first two cations in bacteriorhodopsin bind to similar high-affinity binding sites. Based on these previous studies, it can be safely assumed that Zn^{2+} will bind to the high-affinity binding sites similar to those of Ca^{2+} and Mg^{2+} in bacteriorhodopsin. The XAFS spectral similarity between the 1.0 Zn^{2+}/bR complex and 2.0 Zn^{2+}/bR complex indicates that either the spherical averages of the two high-affinity sites are very similar in terms of the first shell ligands, or that Zn^{2+} has only one type of strong binding site.

The XAFS spectra of Zn^{2+} measured in bR solution are very similar to those measured in wet bR films. As the bR films dry, a substantial structural alteration takes place in which two ligands are lost from the first coordination sphere. The structural change upon drying depends on the concentration of Cl^- ion added during sample preparation. In the absence of Cl^- ions, four N/O ligands are found in the first shell. In the presence of Cl^- ions, however, two N/O and two Cl^-/S^{2-} ligands are found in the first coordination shell. Because no sulfur atoms are present in the system, the contribution can be attributed to two Zn-Cl bonds.

It is important to note that the change observed in going from the dry film state to the wet film state or vice versa is reversible. Radiation damage to the protein sample causing structural changes can thus be ruled out. This suggests that the loss of water molecules can change the local structure of metal cations in bR. Because it is known that no photocycle is observed in dry bR films, in which the structure of the ligands around the metal ion is changed, one is tempted to suggest that the ligated metal ion is not far from the active site. This is consistent with previous observations from neutron scattering that four tightly bound water molecules were found near the PSB (Papadopoulos et al., 1990).

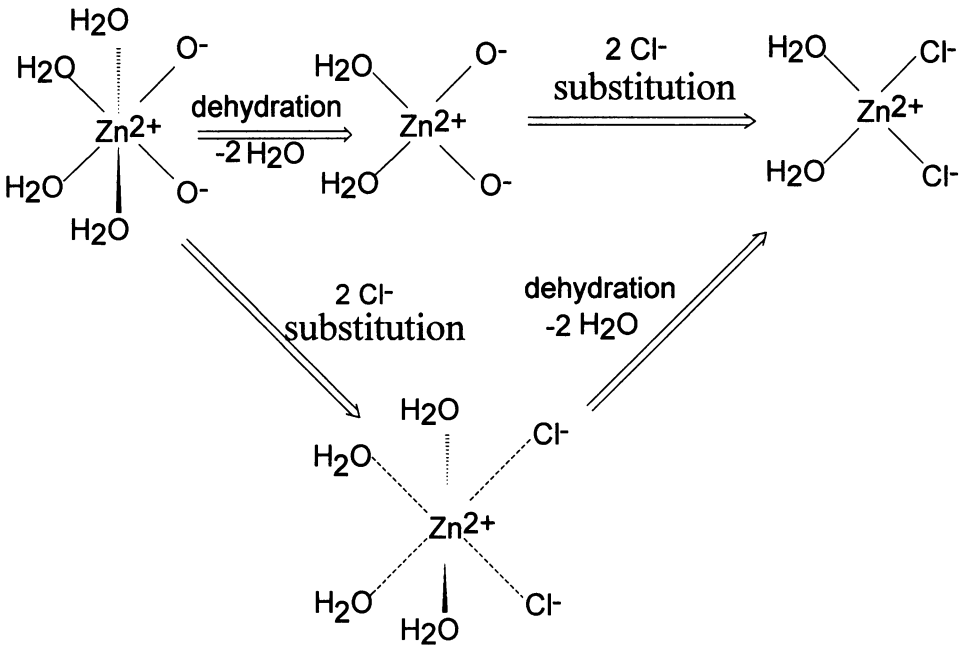

FIGURE 7 Possible mechanisms for the substitution of O^- by Cl^- upon dehydration of the sample in the presence of Cl^- ions. The substitution does not occur in wet bR films or in bR solution.

It can be speculated that two water ligands are dissociated from the zinc ion during drying the bR film, changing the zinc coordination from six to four. When a very low concentration of Cl^- ions is present, the remaining four ligands shift to a shorter average distance between the ligands and the metal cation. When a high concentration of Cl^- ions is present in the system, removing water molecules also causes the replacement of two ligands by the Cl^- ions in the first shell, resulting in the coordination of two N/O ligands and two Cl^- ligands. The observed structural change suggests that two of the ligands are tightly bound and cannot be removed by drying, nor can they be exchanged by Cl^- ions (type I ligands). It also suggests that two weakly bound ligands, which are involved in the binding to Zn^{2+} in regenerated bR solution and wet films, can be removed by drying, and are most likely water molecules (type III ligands). The other two ligands can be displaced by Cl^- ions upon drying in the presence of Cl^- ions (type II ligands). It is tempting to suggest that these two ligands are negatively charged oxygen atoms from an amino acid carboxylate group (or a phosphate group on the phospholipids). When Asp^{85} and D212N are replaced by neutral amino acid residues, Cl^- ions are found to reside (Marti et al., 1992) within the retinal cavity. The addition of anions to the mutants led to the recovery of the proton pump (Marti et al., 1992) and the catalysis of retinal photoisomerization (Logunov et al., 1996). This suggests that ligands of type II are the negatively charged oxygen atoms of the aspartate groups (Asp^{85}, Asp^{212}) within the protein rather than those in the lipid bilayer. This assignment explains why type I ligands are nondissociable and nonexchangeable, as these H_2O molecules around Zn^{2+} are within the protein where the dielectric constant is relatively low. Possible mechanisms for the substitution of O^- by Cl^- upon dehydration of the sample in the presence of Cl^- ions are shown in Fig. 7. It should be emphasized that the structural change (i.e., the replacement of two oxygen ligands by two Cl^- ligands) in the presence of Cl^- ions occurs only upon dehydration of the sample, but not in the wet film or in solution. Two mechanisms are proposed: dehydration followed by substitution or substitution followed by dehydration. The average distance of Cl^- to Zn^{2+} in regenerated dry bR films is 2.29 Å, which is very similar to the average distance of Cl^- to Zn^{2+} in 2 mM $ZnCl_2$ solution, where two Cl^- ligands and four water ligands were found (see Fig. 6) for Zn^{2+}.

To summarize, three types of ligands are found for Zn^{2+} in Zn^{2+}-regenerated bR. Type I ligands are assigned to two strongly bound water molecules. Type II ligands are assigned to two negatively charged ligands, which are most probably the partially negatively charged oxygen atom of aspartate group(s) (Asp^{85} and Asp^{212}). Type III ligands are assigned to weakly bound water molecules.

We thank the Department of Energy, Office of Basic Energy Research (grant DE-FG03-88ER-13828) (Georgia Institute of Technology) and the National Institute of Health (grant GM-47534) (Biostructures Institute) for financial support.

REFERENCES

Ariki, M., and J. K. Lanyi. 1986. Characterization of metal ion-binding sites in bacteriorhodopsin. *J. Biol. Chem.* 261:8167–8174.

Becher, B. M., and J. Y. Cassim. 1975. Improved isolation procedures for the purple membrane of *Halobacterium halobium*. *Prep. Biochem.* 5:161–178.

Braiman, M. S., T. Mogi, T. Marti, L. J. Stern, H. G. Khorana, and K. J. Rothschild. 1988. Vibrational spectroscopy of bacteriorhodopsin mutants: light-driven proton transport involves protonation changes of aspartic acid residues 85, 96, and 212. *Biochemistry.* 27:8516–8520.

Butt, H. J., K. Fendler, E. Bamberg, J. Tittor, and D. Oesterhelt. 1989. Aspartic acids 96 and 85 play a central role in the function of bacteriorhodopsin as a proton pump. *EMBO J.* 8:1657–1663.

Chang, C. H., J. G. Chen, R. Govindjee, and T. Ebrey. 1985. Cation binding by bacteriorhodopsin. *Proc. Natl. Acad. Sci. USA.* 82:396–400.

Chang, C. H., R. Jonas, S. Melchiore, R. Govindjee, and T. G. Ebrey. 1986. Mechanism and role of divalent cation binding of bacteriorhodopsin. *Biophys. J.* 49:731–739.

Chronister, E. L., T. C. Corcoran, L. Song, and M. A. El-Sayed. 1986. On the molecular mechanisms of the Schiff base deprotonation during the bacteriorhodopsin photocycle. *Proc. Natl. Acad. Sci. USA.* 83: 8580–8584.

Corcoran, T. C., K. Z. Ismail, and M. A. El-Sayed. 1987. Evidence for the involvement of more than one metal cation in the Schiff base deprotonation process during the photocycle of bacteriorhodopsin. *Proc. Natl. Acad. Sci. USA.* 84:4094–4098.

Crozier, E. D., J. J. Rehr, and R. R. Ingalls. 1988. Amorphous and liquid systems. *In* X-Ray Absorption: Principle, Application, Techniques of EXAFS, SEXAFS, and XANES. John Wiley and Sons, New York. 373.

Dencher, N. A., J. Heberle, C. Bark, M. H. J. Koch, G. Rapp, D. Oesterhelt, K. Bartels, and G. Bueldt. 1991. Proton translocation and conformational changes during the bacteriorhodopsin photocycle: time-resolved studies with membrane-bound optical probes and x-ray diffraction. *Photochem. Photobiol.* 54:881–887.

Druckmann, S., M. Ottolenghi, A. Pande, J. Pande, and R. H. Callender. 1982. Acid-base equilibrium of the Schiff base in bacteriorhodopsin. *Biochemistry.* 21:4953–4959.

Dunach, M., E. Padros, M. Seigneuret, and J. L. Rigaud. 1988a. On the molecular mechanism of the blue to purple transition of bacteriorhodopsin. UV-difference spectroscopy and electron spin resonance studies. *J. Biol. Chem.* 263:7555–7559.

Dunach, M., M. Seigneuret, J. L. Rigaud, and E. Padros. 1987. Characterization of the cation binding sites of the purple membrane. Electron spin resonance and flash photolysis studies. *Biochemistry.* 26:1179–1186.

Dunach, M., M. Seigneuret, J. L. Rigaud, and E. Padros. 1988b. Influence of cations on the blue to purple transition of bacteriorhodopsin. Comparison of calcium and mercury(2+) binding and their effect on the surface potential. *J. Biol. Chem.* 263:17378–17384.

Englehard, M., B. Hess, M. Chance, and B. Chance. 1987. X-ray absorption studies on bacteriorhodopsin. *FEBS Lett.* 222:275–278.

Griffiths, J. A., J. King, R. Browner, and M. A. El-Sayed. 1996a. Calcium and magnesium binding in native and structurally perturbed purple membrane. *J. Phys. Chem.* 100:929–933.

Griffiths, J. A., T. M. Masciangioli, C. Roselli, and M. A. El-Sayed. 1996b. Monodentate vs bidentate binding of lanthanide cations to PO_2^- in bacteriorhodopsin. *J. Phys. Chem.* 100:6863–6866.

Heberle, J., and N. A. Dencher. 1992. Surface-bound optical probes monitor proton translocation and surface potential changes during the bacteriorhodopsin photocycle. *Proc. Natl. Acad. Sci. USA.* 89:5996–6000.

Horrocks, W. D., J. N. Isheley, B. Holmquist, and J. S. Thompson. 1980. Structural and electronic mimics of the active site of cobalt (II)-substituted zinc metalloezymes. *J. Inorg. Chem.* 12:131–141.

Jonas, R., and T. G. Ebrey. 1991. Binding of a single divalent cation directly correlates with the blue-to-purple transition in bacteriorhodopsin. *Proc. Natl. Acad. Sci. USA.* 88:149–153.

Katre, N. V., Y. Kimura, and R. M. Stroud. 1986. Cation binding sites on the projected structure of bacteriorhodopsin. *Biophys. J.* 50:277–284.

Kobayashi, T., H. Ohtani, J. Iwai, A. Ikegami, and H. Uchiki. 1983. Effect of pH on the photoreaction cycles of bacteriorhodopsin. *FEBS Lett.* 162:197–200.

Lee, P. A., P. H. Citrin, P. Eisenberger, and B. M. Kincaid. 1981. Extended x-ray absorption fine structure: its strength and limitations as a structural tool. *Rev. Mod. Phys.* 53:769–806.

Logunov, S. L., M. A. El-Sayed, and J. K. Lanyi. 1996. Catalysis of the retinal subpicosecond process in acid purple bacteriorhodopsin and some bacteriorhodopsin mutants by chloride ions. *Biophy. J.* 71:1545–1553.

Lozier, R. H., W. Niederberger, R. A. Bogomolni, S. B. Hwang, and W. Stoeckenius. 1976. Kinetics and stoichiometry of light-induced proton release and uptake from purple membrane fragments, *Halobacterium halobium* cell envelopes and phospholipid vesicles containing oriented purple membrane. *Biochim. Biophys. Acta.* 440:545–556.

Marti, T., H. Otto, S. J. Rosselet, M. P. Heyn, and H. G. Khorana. 1992. Anion binding to the Schiff base of bacteriorhodopsin mutants Asp-85→Asp/Asp-212→Asn and Arg-82→Gln/Asp-85→Asn/Asp-212→Asn. *J. Biol.Chem.* 267:16922–16927.

Mitra, A. K., and R. M. Stroud. 1990. High sensitivity electron diffraction analysis. A study of divalent cation binding to purple membrane. *Biophys. J.* 57:301–311.

Mustre de Leon, J., J. J. Rohr, S. L. Zabinsky, and R. C. Albers. 1991. Ab initial curved-wave x-ray-absorption fine structure. *Phys. Rev. B.* 44: 4146–4156.

Oesterhelt, D., and W. Stoeckenius. 1971. Rhodopsin-like protein from the purple membrane of *Halobacterium halobium. Nature New Biol.* 233: 149–152.

Oesterhelt, D., and W. Stoeckenius. 1974. Isolation of the cell membrane of *Halobacterium halobium* and its fractionation into red and purple membrane. *Methods Enzymol.* 31:667–678.

Ort, D. R., and W. W. Parson. 1978. Flashed-induced volume changes of bacteriorhodopsin-containing membrane fragments and their relationship to proton movements and absorbance transients. *J. Biol. Chem.* 253:6158–6164.

Otto, H., T. Marti, M. Holz, T. Mogi, L. J. Stern, F. Engel, H. G. Khorana, and M. P. Heyn. 1990. Substitution of amino acids Asp-85, Asp-212, and Arg-82 in bacteriorhodopsin affects the proton release phase of the pump and the pK of the Schiff base. *Proc. Natl. Acad. Sci. USA.* 87:1018–1022.

Papadopoulos, G., N. A. Dencher, G. Zaccai, and G. Bualdt. 1990. Water molecules and exchangeable hydrogen ions at the active center of bacteriorhodopsin localized by neutron diffraction: elements of the proton pathway? *J. Mol. Biol.* 214:15–19.

Petersheim, M., H. N. Halladay, and J. Blodnicks. 1989. Tb^{3+} and Ca^{2+} binding to phosphatidylcholine. A study comparing data from optical, NMR, and infrared spectroscopies. *Biophys. J.* 56:551–557.

Roselli, C., A. Boussac, T. A. Mattioli, J. A. Griffiths, and M. A. El-Sayed. 1996. Detection of Yb^{3+} binding site in regenerated bacteriorhodopsin that is coordinated with the protein and the phospholipid head groups. *Proc. Natl. Acad. Sci. USA.* 93:14333–14337.

Sepulcre, F., J. Cladera, J. Garcia, M. G. Proietti, J. Torres, and E. Padros. 1996. An extended X-ray absorption fine structure study of the high-affinity cation-binding site in the purple membrane. *Biophys. J.* 70: 852–856.

Sheves, M., A. Albeck, N. Friedman, and M. Ottolenghi. 1986. Controlling the pKa of the bacteriorhodopsin Schiff base by use of artificial retinal analogs. *Proc. Natl. Acad. Sci. USA.* 83:3262–3266.

Stern, E. A., Y. Ma, O. Hanske-Petitpierre, and C. E. Bouldin. 1992. Radial distribution function in x-ray-absorption fine structure. *Phys. Rev. B.* 46:687–694.

Stuart, J. A., B. W. Vought, C. Zhang, and R. R. Birge. 1995. The active site of bacteriorhodopsin. Two-photon spectroscopic evidence for a positively charged chromophore binding site mediated by calcium. *Biospectroscopy.* 1:9–28.

Sweetman, L. L., and M. A. El-Sayed. 1991. The binding site of the strongly bound europium(3+) in europium(3+)-regenerated bacteriorhodopsin. *FEBS Lett.* 282:436–440.

Szundi, I., and W. Stoeckenius. 1987. Effect of lipid surface charges on the purple-to-blue transition of bacteriorhodopsin. *Proc. Natl. Acad. Sci. USA.* 84:3681–3684.

Szundi, I., and W. Stoeckenius. 1988. Purple-to-blue transition of bacteriorhodopsin in a neutral lipid environment. *Biophys. J.* 54:227–232.

Szundi, I., and W. Stoeckenius. 1989. Surface pH controls purple-to-blue transition of bacteriorhodopsin. A theoretical model of purple membrane surface. *Biophys. J.* 56:369–383.

Webster, L. C., K. Zhang, B. Chance, I. Ayene, J. S. Culp. W. Huang, F. Y. Wu, and R. P. Ricciadi. 1991. Conversion of the E1A Cys_4 zinc finger to a nonfunctional His_2 : Cys_2 zinc finger by a single point mutation. *Proc. Natl. Acad. Sci. USA.* 88:9989–9993.

Yoo, S.-K., E. S. Awad, and M. A. El-Sayed. 1995. Comparison between the binding of Ca^{2+} and Mg^{2+} to the two high-affinity sites of bacteriorhodopsin. *J. Phys. Chem.* 99:11600–11604.

Zhang, K., B. Chance, D. S. Auld, K. S. Larsen, and B. L. Vallee. 1992a. X-ray absorption fine structure study of the active site of zinc and cobalt carboxypeptidase A in their solution and crystalline forms. *Biochemistry.* 31:1159.

Zhang, K. E., A. Stern, F. Ellis, J. Sanders-Loehr, and A. K. Shiemke. 1988. The active site of hemerythrin as determined by x-ray absorption fine structure. *Biochemistry.* 27:7470–7479.

Zhang, K., G. Rosenbaum, and G. Bunker. 1992b. The correction of the dead time loss of the Ge detector in x-ray absorption spectroscopy. *Jpn. J. Appl. Phys.* 32(Suppl. 32-2):147–149.

Zhang, N. Y., and M. A. El-Sayed. 1993. The C-terminus and the calcium low-affinity binding sites in bacteriorhodopsin. *Biochemistry.* 32: 14173–14175.

Zhang, N. Y., M. A. El-Sayed, M. L. Bonet, J. K. Lanyi, M. Chang, B. Ni, and R. Needleman. 1993. Effects of genetic replacements of charged and hydrogen-bonding residues in the retinal pocket on calcium binding to deionized bacteriorhodopsin. *Proc. Natl. Acad. Sci. USA.* 90:1445–1449.

Zhang, N. Y., L. L. Sweetman, E. S. Awad, and M. A. El-Sayed. 1992. Nature of the individual calcium binding sites in Ca^{2+}-regenerated bacteriorhodopsin. *Biophys. J.* 61:1201–1206.